

# ESTIMATION OF THE TOTAL SLIDING DISTANCE OF COMPOSITE TYPE BREAKWATER IN SERVICE PERIOD APPLYING THE WAVE CLIMATE STATISTICS

Teruko Kimura<sup>1</sup>, Akira Kimura<sup>2</sup> and Takao Ota<sup>3</sup>

Since 2007, damages of structures are accepted if they give less influence on their performance in Japan (Guideline for the performance design). To realize the idea of the guideline in a coastal structure design, assessment for 'state' and 'degree' of damage becomes essential in advance. This study proposes statistical method to assess a sliding of the composite breakwater, applying Monte Carlo wave climate simulation method (kimura et al., 2012). A concrete method is shown to make clear about a relation between design conditions and a probability that the structure keeps the performance during the in-service period.

*Keywords: performance based design; composite type breakwater; sliding distance; wave climate statistics*

## Introduction

In 2007, the guideline of the design scheme for public structures was changed from a conventional detailed specification design to a performance design in Japan. Slight damage of a structure came to be accepted in the new guideline as long as the demanded performance is maintained. It becomes possible to design the structure considering repairs during the in-service period. A flexible cost planning becomes possible. It becomes necessary that the 'scales' and 'frequency' of damages during the in-service period are statistically clear in advance. It is preferable that the repair strategy is also included in the overall planning. The present study selected the sliding of breakwater as an example of the structure damage. Statistical method is shown to estimate the sliding distance of a composite breakwater applying the wave climate statistics. Shimosako and Takahashi (1998) studied expected sliding distance of a composite breakwater during the in-service period. They used the extreme value (annual maximum wave height) statistics. From the statistical restriction they exerted waves to the breakwater only 2 hours every year during the in-service period. Since the present study used a wave climate statistics (Kimura and Ota, 2012), all waves act on the breakwater during its in-service period are taken into account in the calculation of its sliding distance. The scheme to simulated Probability Distribution Function (PDF) of the one year and the longer years sliding distances are explained in this study. Examples of the the 'timing' of repairs are shown in the last.

## Wave climate statistics

Monte Carlo wave climate simulation is briefly reviewed as follows (Kimura and Ota, 2012). Wave climate data observed along the Sea of Japan coast (7 observatories) are used as targets of the simulations. Figure 1 shows an example of the one year observed significant wave heights  $H_{1/3}$  (every 2 hours : Rumoi 2001; NOWPHAS). Numbers on the horizontal axis show days counted from Jan. 1<sup>st</sup>. Wave conditions are stormy in winter but very quite in summer in the Sea of Japan. Figure 2 shows a Fourier spectrum  $|F'(f_n)|$  of  $H_{1/3}$  (Fig.1). Regardless of the observatories,  $|F'(f_n)|$  has a similar properties. According to the properties of  $|F'(f_n)|$ , the spectrum can be divided into 3 frequency regions as shown in Table 1.

| Region | $f_n$ (d <sup>-1</sup> ) | Property   |
|--------|--------------------------|--|
| A      | ~0.006                   | Rapid attenuation of $ F'(f_n) $ according to an increase of the frequency $f_n$ |
| B      | 0.006~0.2                | Almost constant $ F'(f_n) $ regardless of $f_n$                                  |
| C      | 0.2~                     | $ F'(f_n) $ attenuates almost proportional to $f_n^{-1}$                         |

in which d means one day. The frequency  $f_n$  is determined as  $f_n = n/365$  [d<sup>-1</sup>], ( $n = 0,1, \dots, 365 \times 12$ ).  $F'(f_n)$  is approximated using the properties shown in the Table 1. In the region A, the values of  $F'(f_n)$  are used. In the regions B and C,  $|F'(f_n)|$  is approximated as

$$\left. \begin{array}{l} \text{Region B:} \\ \text{Region C:} \end{array} \right\} \begin{array}{l} |F'(f_n)|_B = c_1 \\ |F'(f_n)|_C = c_2 f_n^{-1} \end{array} \quad (1)$$

in which  $c_1$  and  $c_2$  are constants.

<sup>1</sup> Senior IT specialist

<sup>2</sup> NEWJEC

<sup>3</sup> Associate Prof. Tottori University

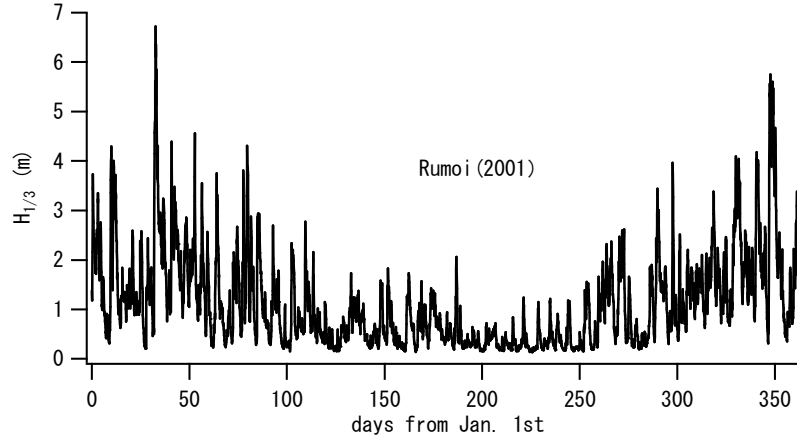


Figure 1. Example of the one year observed significant wave heights  $H_{1/3}$  (every 2 hours : Rumoi 2001; NOWPHAS).

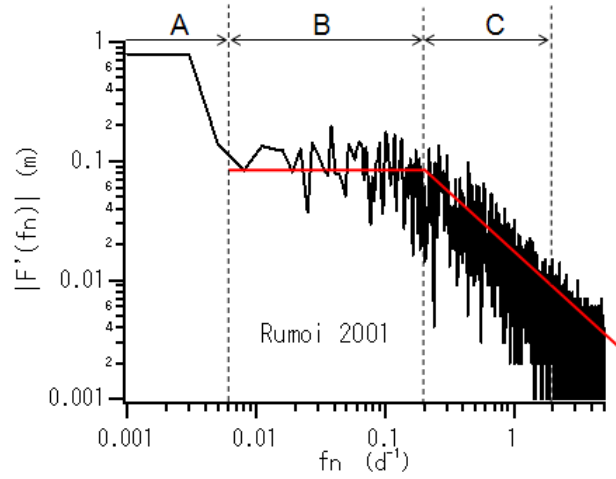


Figure 2. Fourier spectrum  $|F'(f_n)|$  of  $H_{1/3}$  (Fig.1).

$H_{1/3}(t_i)$  with time interval  $dt$  is simulated as follows.

$$H_{1/3}(t_i) = H_A(t_i) \times \left\{ 1 + \sum_{n1=3}^{73} (\bar{c}_1 + c_{\sigma 1} R_{n1}) \cos(2\pi f_{n1} t_i + \varepsilon_{n1}) + \sum_{n2=74}^{731} (\bar{c}_2 + c_{\sigma 2} R_{n2}) f_{n2}^{-1} \cos(2\pi f_{n2} t_i + \varepsilon_{n2}) \right\} \quad (2)$$

$$\left. \begin{aligned} t_i &= idt \\ \varepsilon_{n1} &= 2\pi R_{Un1}, \quad \varepsilon_{n2} = 2\pi R_{Un2} \end{aligned} \right\} \quad (3)$$

where

$$H_A(t_i) \approx \bar{H}_A(t_i) + H_{\sigma}(t_i) R_{n3i} \quad (4)$$

$$\bar{H}_A(t_i) = \frac{1}{2} \bar{a}_0 + \sum_{n=1}^2 \{ \bar{a}_n \sin 2\pi f_n t_i + \bar{b}_n \cos 2\pi f_n t_i \} \quad (5)$$

$$H_{\sigma}(t_i) = \left\{ \frac{1}{M} \sum_{m=1}^M [H_{Am}(t_i) - \bar{H}_A(t_i)]^2 \right\}^{1/2} \quad (6)$$

$$(i = 1, 2, \dots, 365 \times 12)$$

in which  $\bar{c}_1$  and  $\bar{c}_2$  are the averaged values of the approximated  $c_1$  and  $c_2$  (Eq. 1) for the observed  $|F'(f_n)|_B$  and  $|F'(f_n)|_C$  every year from 1991 to 2008 (18 years).  $c_{\sigma 1}$  and  $c_{\sigma 2}$  are the standard deviation of  $c_1$  and  $c_2$ , respectively.  $R_{n1}$ ,  $R_{n2}$  and  $R_{n3i}$  are mutually independent normal random numbers with  $N(0,1)$ .  $R_{Un1}$  and  $R_{Un2}$  are also independent uniform [0~1] random number.  $\bar{H}_A(t_i)$  is the  $M$  years average of  $H_A(t_i)$ , ( $i = 1, 2, \dots, 4380 (= 365 \times 12)$ ).  $a_0$ ,  $a_1$ ,  $a_2$ ,  $b_1$  and  $b_2$  are the real and imaginary parts of the Fourier components ( $a_i = \text{Re}(F'(f_n))$ ,  $b_i = \text{Im}(F'(f_n))$ ). Over bar means an average over observation years  $M$ .

| Table 2 Constants for the simulations (Kimura and Ota, 2012). |         |         |         |         |         |         |         |
|---|---------|---------|---------|---------|---------|---------|---------|
|   | Rumoi   | Setana  | Akita   | Niigata | Wajima  | Tottori | Hamada  |
| $\bar{a}_0$   | 1.119   | 1.188   | 1.088   | 1.000   | 1.197   | 1.093   | 1.119   |
| $\bar{a}_1$   | 0.777   | 0.805   | 0.680   | 0.726   | 0.777   | 0.650   | 0.597   |
| $\bar{b}_1$   | 0.093   | 0.088   | 0.144   | 0.106   | 0.093   | 0.062   | 0.081   |
| $\bar{a}_2$   | 0.150   | 0.057   | 0.120   | 0.142   | 0.150   | 0.101   | 0.091   |
| $\bar{b}_2$   | 0.067   | -0.022  | 0.020   | 0.077   | 0.067   | 0.078   | 0.083   |
| $\bar{H}_\sigma$  | 0.107   | 0.120   | 0.138   | 0.108   | 0.129   | 0.111   | 0.123   |
| $\bar{c}_1$   | 0.0818  | 0.0817  | 0.1000  | 0.0824  | 0.0741  | 0.0777  | 0.0778  |
| $c_{\sigma 1}$  | 0.00718 | 0.00594 | 0.00860 | 0.00634 | 0.00462 | 0.00557 | 0.00722 |
| $\bar{c}_2$   | 0.0155  | 0.0150  | 0.0184  | 0.0157  | 0.0130  | 0.0134  | 0.0137  |
| $c_{\sigma 2}$  | 0.00093 | 0.00085 | 0.00150 | 0.00107 | 0.00101 | 0.00105 | 0.00128 |

Unit: m/d:  $\bar{c}_2$ ,  $c_{\sigma 2}$ , m: otherwise.

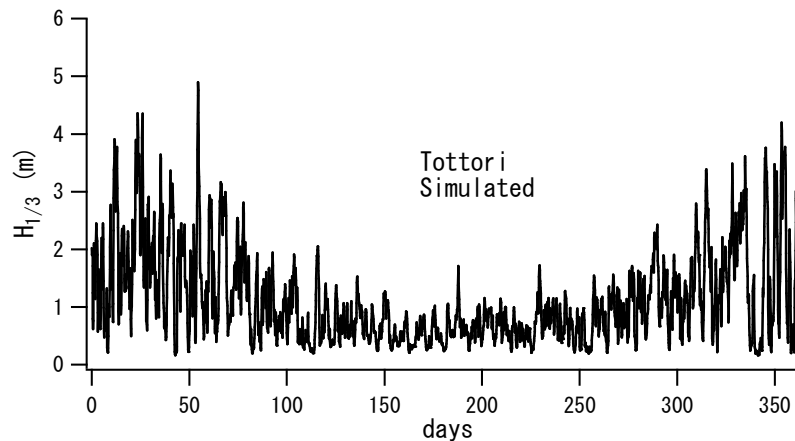


Figure 3. Simulated one year  $H_{1/3}$  (Tottori).

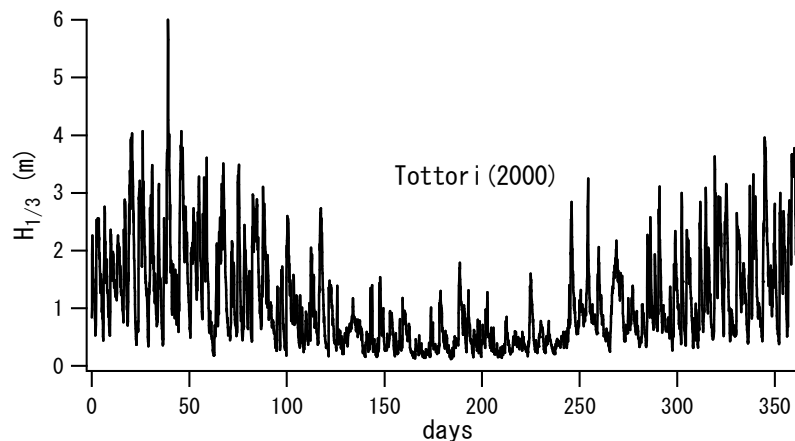


Figure 4. Observed  $H_{1/3}$  (Tottori, 2000)

Standard deviations for  $a_0$ ,  $a_1$ ,  $a_2$ ,  $b_1$ , and  $b_2$  are negligibly small for  $i$  in Eq.(5).  $H_\sigma(t_i) \approx \bar{H}_\sigma$ . Figure 3 shows a simulated one year  $H_{1/3}$  (Tottori). Figure 4 shows an observed  $H_{1/3}$  (Tottori, 2000).

However, 2~3 % of entire simulated  $H_{1/3}$  (Eqs.(2) ~ (6)) have negative values. In the former study (Kimura and Ota, 2012), one method to correct this property was explained using a skew symmetric function. A modified correction method without the function is explained here. The simulated  $H_{1/3}$  is converted to  $(H_{1/3})_{con}^1$  so that they satisfy Eq.(7) to correct the negative value problem.

$$F_{obs}[(H_{1/3})_{con}^1] = F_{sim}[H_{1/3}] \quad (7)$$

in which  $F_{obs}[\ ]$  and  $F_{sim}[\ ]$  are cumulative frequency distributions of observed and simulated  $H_{1/3}$ . This method is effective if there are large number of observed data. If an agreement between the cumulative distributions of the converted  $F_{con}^1[(H_{1/3})_{con}^1]$  and  $F_{obs}[H_{1/3}]$  is insufficient, repetition of the conversion improves the result.

$$F_{obs}[(H_{1/3})_{con}^n] = F_{con}^{n-1}[(H_{1/3})_{con}^{n-1}] \quad (n = 2, 3, \dots) \quad (8)$$

in which  $(H_{1/3})_{con}^{n-1}$  is the  $n-1$  times converted value and  $F_{con}^{n-1}[(H_{1/3})_{con}^{n-1}]$  is its cumulative distribution. Two or three times conversions ( $n = 2, 3$ ) give very good result. In the high end of the frequency distributions of observed and simulated  $H_{1/3}$ , uneven properties appear due to data shortage. Exponential function of the type  $ae^{-bH_{1/3}}$  gives good approximation of their frequency distributions in the large  $H_{1/3}$  region (Kimura and Ota, 2012, 2013) in which  $a$  and  $b$  are constants. Figure 5 shows an example of the frequency distributions of  $(H_{1/3})_{con}^3$  (black line) and observed  $H_{1/3}$  (+) (Tottori).

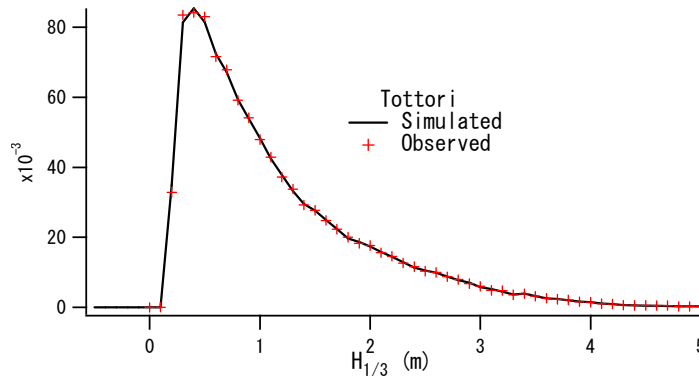


Figure 5. Example of the frequency distributions of  $(H_{1/3})_{con}^3$  (black line) and observed  $H_{1/3}$  (+) (Tottori).

Detailed statistical properties of  $(H_{1/3})_{con}^n$  are in good agreements with the observed values (Kimura and Ota, 2013).

#### Sliding distance of composite breakwater

Studies on coastal structures have mainly aimed at clarifying the start of damages (limit states) to meet with the ordinary design manual (detailed specification design). Very few studies deal with the behavior of structures after the damages start. There is a flow of the studies on the breakwater damage started by Ito (1971). Shimosako and Takahashi (1994) and Tanimoto et al. (1996) are the studies follow the flow. These studies together with a wave pressure model by Goda (1974) are the very few examples treated the behavior after the damage (sliding) starts. The present study applies their models to study the long period statistical property of a sliding distance of the composite breakwater. The study by Shimosako and Takahashi (1998) on the composite breakwater sliding is briefly reviewed as follows.

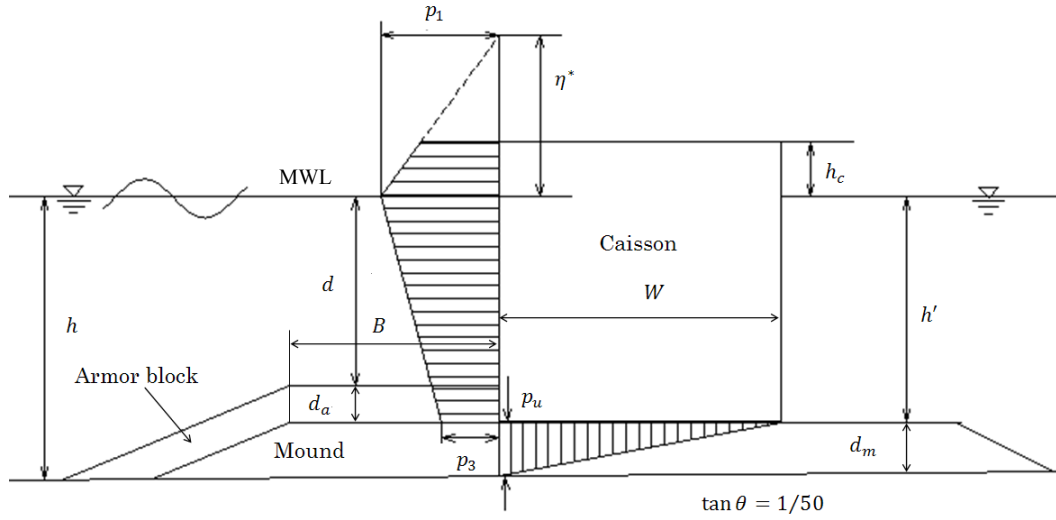


Figure 6. Model composite type breakwater.

Figure 6 shows the model composite breakwater. Vertical wave pressure distribution is approximated by a trapezoid (below the mean water level MWL) and a triangle (above MWL, height :  $\eta^*$ ) (Goda, 1974 : Fig.6). Wave pressures at the MWL and the bottom of the caisson are given by  $p_1$  and  $p_3$ . If the crest height of the breakwater is lower than  $\eta^*$ , pressure above the crest is ignored (Fig.6). The whole wave pressure  $P$  is given by

$$P = \frac{1}{2}(p_1 + p_3)h' + \frac{1}{2}(p_1 + p_4)h_c^* \quad (9)$$

where

$$p_1 = (\alpha_1 + \alpha^*)\rho_w gH, \quad \alpha^* = \max\{\alpha_2, \alpha_1\} \quad (10)$$

$$p_3 = \alpha_3 p_1 \quad (11)$$

$$p_4 = \begin{cases} p_1(1 - h_c/\eta^*) & : \eta^* > h_c \\ 0 & : \eta^* \leq h_c \end{cases} \quad (12)$$

in which

$$\left. \begin{aligned} h_c^* &= \min\{\eta^*, h_c\} \\ \eta^* &= 1.5H \\ \alpha_1 &= 0.6 + \frac{1}{2} \left[ \frac{4\pi h/L}{\sinh(4\pi h/L)} \right]^2 \\ \alpha_2 &= \min \left\{ \frac{h_* - d}{3h_*} \left( \frac{H}{d} \right)^2, \frac{2d}{H} \right\} \\ \alpha_3 &= 1 - \frac{h'}{h} \left[ 1 - \frac{1}{\cosh(2\pi h/L)} \right] \end{aligned} \right\} \quad (13)$$

$$\left. \begin{aligned} \alpha_1 &= \alpha_{1,0} \cdot \alpha_{1,1} \\ \alpha_{1,0} &= \min \left\{ \frac{H}{d}, 2.0 \right\} \\ \alpha_{1,1} &= \begin{cases} \cos \delta_2 / \cosh \delta_1 & : \delta_2 \leq 0 \\ 1 / [\cosh \delta_1 \times \cosh^{0.5} \delta_2] & : \delta_2 > 0 \end{cases} \\ \delta_1 &= \begin{cases} 20\delta_{11} & : \delta_{11} \leq 0 \\ 15\delta_{11} & : \delta_{11} > 0 \end{cases} \\ \delta_2 &= \begin{cases} 4.9\delta_{22} & : \delta_{22} \leq 0 \\ 3.0\delta_{22} & : \delta_{22} > 0 \end{cases} \end{aligned} \right\} \quad (14)$$

$$\left. \begin{aligned} \delta_{11} &= 0.93 \left( \frac{B}{L} - 0.12 \right) + 0.36 \left( 0.4 - \frac{d}{h} \right) \\ \delta_{22} &= -0.36 \left( \frac{B}{L} - 0.12 \right) + 0.93 \left( 0.4 - \frac{d}{h} \right) \end{aligned} \right\} \quad (15)$$

in which  $H$  and  $L$  are the wave height and the wave length,  $h$  is the water depth,  $h_c$  is the height of the breakwater crest above MWL,  $d$  is the water depth on the covering on the mound,  $B$  is the front width of the mound top,  $\rho_w$  is the water density,  $g$  is the gravitational acceleration. All waves act at right angle to the breakwater.  $\eta^* = 1.5H_{max}$  (Eq.(13)) and  $h_*$  is the water depth at  $5H_{1/3}$  off the breakwater in the original model (Goda, 1975) and  $H_{max} = 1.8H_{1/3}$ . Since all waves are handled individually in the present study,  $5H$  and  $H$  are used instead of  $5H_{1/3}$  and  $H_{max}$ , respectively. Since a shock wave pressures effects is taken into account in the present study, next improved model by Shimosaki et al. is applied. Their whole wave pressure  $P$  is given by

$$P(t) = \max\{P_1(t), P_2(t)\} \quad (16)$$

$$P_1(t) = \gamma_p (P_1)_{max} \sin \frac{2\pi t}{T} \quad (17)$$

$$P_2(t) = \begin{cases} \frac{2t}{\tau_0} (P_2)_{max} & : 0 \leq t \leq \frac{\tau_0}{2} \\ 2 \left(1 - \frac{t}{\tau_0}\right) (P_2)_{max} & : \frac{\tau_0}{2} < t \leq \tau_0 \\ 0 & : \tau_0 < t \end{cases} \quad (18)$$

$$\gamma_p = 1 - \frac{\pi}{(P_1)_{max} T} \int_{t_1}^{t_2} \left[ P_2(t) - (P_1)_{max} \sin \frac{2\pi t}{T} \right] dt \quad (19)$$

$$: P_2(t) - (P_1)_{max} \sin 2\pi t/T \geq 0$$

in which  $(P_1)_{max}$  is the horizontal whole pressure (Eq.(9)) (only  $\alpha_1$  is considered in Eq.(10)),  $(P_2)_{max}$  is also the horizontal whole pressure, (only  $\alpha^*$  is considered in Eq.(10)). Figure 7 shows a shock wave pressure model shown by Tanimoto et al. (1996).

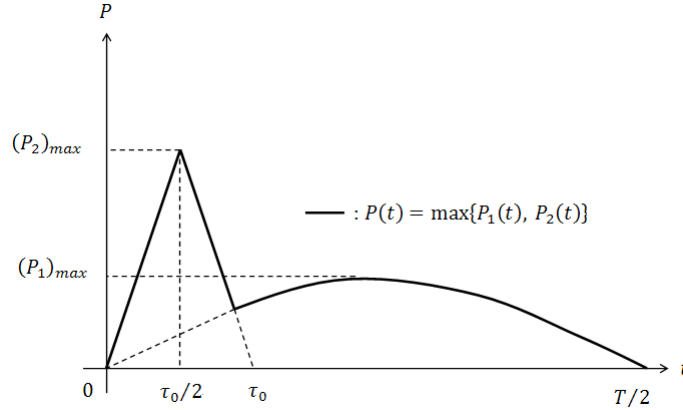


Figure 7. Shock wave pressure model shown by Tanimoto et al. (1996).

The mild curve  $(P_1(t))$ : Fig.7) shows a standing wave pressure and the triangle shows a shock pressure  $(P_2(t))$ : Fig.7).  $(P_1)_{max}$  and  $(P_2)_{max}$  are their maximum values.  $T$  is the wave period and  $\tau_0$  is the duration of the shock pressure given by,

$$\tau_0 = k\tau_{0,F} \quad (20)$$

$$\tau_{0,F} = \begin{cases} \left(0.5 - \frac{H}{8h}\right)T & : 0 < \frac{H}{h} \leq 0.8 \\ 0.4T & : 0.8 < \frac{H}{h} \end{cases}, \quad k = [(\alpha^*)^{0.3} + 1]^{-2} \quad (21)$$

Equation of motion of the breakwater is given by

$$\left(\frac{W_a}{g} + M_a\right) x_G'' = P - F_R \quad (22)$$

$$\left. \begin{aligned} M_a &\approx 1.086\rho_w h^2 \\ F_R &= \mu[(W_a - W_w) - U] \end{aligned} \right\} \quad (23)$$

in which  $x_G$  is the sliding distance of the caisson, " means  $d/dt^2$ ,  $W_a$  is a weight of the caisson in the air,  $M_a$  is an added mass of the breakwater in the water,  $P$  is given by Eq.(16),  $F_R$  is the friction

force,  $\mu$  is the friction coefficient between the caisson and the mound,  $W_w$  is the buoyancy of the caisson,  $U$  is the lift force acting on the caisson given by,

$$U = \frac{1}{2} p_u B \quad (24)$$

$$p_u = \alpha_1 \alpha_3 \rho_w g H \quad (25)$$

Solving Eq.(22), sliding distance  $s$  by the wave with  $H$  and  $L$  (and  $T$ ) is given by,

$$s = \frac{g \tau_0^2 (F_s - \mu W_e)^3 (F_s + \mu W_e)}{8 \mu W_a W_e F_s^2} \quad (26)$$

in which  $F_s = P_{max} + U$  and  $W_e = W_a - W_w$ ,  $P_{max}$  is the maximum value of  $P(t)$  (Eq.(16), both  $\alpha_1$  and  $\alpha^*$  in Eq.(10) are taken into account).

### Probability distribution function of the sliding distances

It is possible to consider wave breaking effects in the wave pressure model (Eq.(10)). Therefore information about the breaking/non-breaking of individual waves included in the waves represented by  $H_{1/3}$  (calculated by Eq.(2)) is required. Applying the Goda model (1975), status of wave (breaking / non-breaking) is identified statistically. Waves arriving at the breakwater are assumed statistically stationary during  $T_L$  (2 hours observation interval for example).

Changes in wave height due to shoaling is calculated applying the linear wave theory.

$$(H_{1/3}; T_{1/3})_{sim} \rightarrow (H_{1/3}; T_{1/3})_0 \rightarrow (H_{1/3}; T_{1/3})_h$$

in which  $( )_{sim}$ ,  $( )_0$  and  $( )_h$  are the values at the wave observatory (wave gauge point), deep water and the breakwater, respectively.

Since the wave period  $T$  distribute around  $T_{1/3}$  when  $H > \bar{H}$  ( $\bar{H}$  : mean wave height) in the joint distribution of observed  $H$  and  $T$  (Goda, 2010).  $T_{1/3}$  distribute around  $\bar{T}_{1/3}$  when  $H_{1/3}$  is large in the joint PDF of  $H_{1/3}$  and  $T_{1/3}$  (Kimura and Ota, 2014). Sliding of the breakwater takes place only when wave height  $H$  is very large.  $\bar{T}_{1/3}$  is, therefore, approximately used for the period ( $T$ ) of individual waves in this study. This approximation about the period may not be too rough. If detailed investigation is necessary, better approximation using joint PDFs of  $H_{1/3}$  and  $T_{1/3}$  and  $H$  and  $T$  is possible (Kimura and Ota, 2014).

Breaking wave height  $H_b$  at the water depth  $h$  is given by the next equation (Goda, 1975).

$$\frac{H_b}{L_0} = A \left\{ 1 - \exp \left[ -1.5 \frac{\pi h}{L_0} (1 + 15 \tan^{4/3} \theta) \right] \right\} \quad (27)$$

in which  $L_0$  is the deep water wave length,  $\tan \theta$  is the sea bottom slope. Since Eq.(27) has some uncertainty for  $H_b$ , Goda introduced the selective breaking probability  $P_B(H)$  to cope with the uncertainty.

$$P_B(H) = \begin{cases} 0 & : H < H_1 \\ (H - H_1)/(H_2 - H_1) & : H_1 \leq H \leq H_2 \\ 1 & : H > H_2 \end{cases} \quad (28)$$

$H_1$  and  $H_2$  are given by Eq.(27) putting  $A = 0.12$  and  $0.18$ , respectively.

PDF of wave height in the deep water condition with  $(H_{1/3})_0$  is calculated (Rayleigh distribution).  $H_1$  and  $H_2$  are converted to the wave heights in deep water condition as,

$$H_{i0} = H_i / K_s \quad (i = 1, 2) \quad (29)$$

Figure 8 shows the PDFs of wave heights which are breaking and non-breaking in deep water condition. Solid and broken lines show the PDFs of non-breaking ( $P_{nbo}(H_0)$ ) and breaking ( $P_{bo}(H_0)$ ) waves, respectively ( $H_{1/3} = 6$  m,  $\bar{T}_{1/3} = 8.95$  s,  $h = 15$  m,  $\tan \theta = 1/50$ ).

Wave height in the position of the breakwater is given as follows (Goda, 1975).

Non-breaking wave (solid line in Fig.8) :

$$H = C_\alpha K_s (H_{1/3})_0 \quad (30)$$

Breaking wave (broken line in Fig.8) :

$$H = \frac{C_\alpha}{1.8} \min \{ (\beta_0 (H_{1/3})_0 + \beta_1 h), \beta_{max} (H_{1/3})_0 \} \quad (31)$$

where

$$\left. \begin{aligned} \beta_0 &= \left\{ 0.052 \left( \frac{(H_{1/3})_0}{(L_{1/3})_0} \right)^{-0.39} \times \exp[20 \tan^{1.5} \theta] \right\} \\ \beta_1 &= 0.63 \exp[3.8 \tan \theta] \\ \beta_{max} &= \max \left\{ 1.65, 0.53 \left( \frac{(H_{1/3})_0}{(L_{1/3})_0} \right)^{-0.29} \right. \\ &\quad \left. \times \exp[2.4 \tan \theta] \right\} \end{aligned} \right\} \quad (32)$$

in which  $C_\alpha$  in Eqs.(30) and (31) is a constant to give an arbitral wave height in deep water condition ( $H_0 = C_\alpha (H_{1/3})_0$ ).

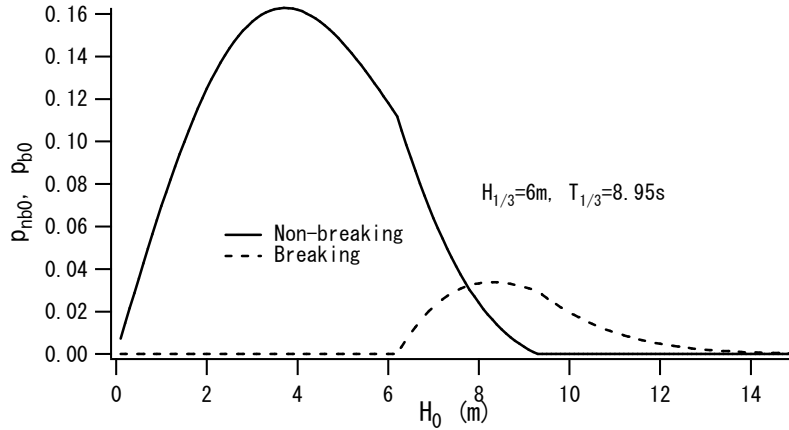


Figure 8. PDFs of wave heights which are breaking and non-breaking in the depth position of the breakwater.

Total number of waves during  $T_L$  is  $NW = T_L \times 3600 / \bar{T}_{1/3}$ . Number of waves with  $H_0 = C_\alpha (H_{1/3})_0$  in the deep water condition is given as,

Non breaking :

$$P_{nb0} \left( C_\alpha (H_{1/3})_0 \right) dH_0 \cdot NW \quad 0 < H_0 \leq H_{i2} \quad (33)$$

Breaking :

$$P_{b0} \left( C_\alpha (H_{1/3})_0 \right) dH_0 \cdot NW \quad H_0 \geq H_{i1} \quad (34)$$

Sliding distance is calculated substituting the converted wave height  $H$  from  $H_0$  and wave period  $\bar{T}_{1/3}$  in equations from Eq.(9) to Eq.(26). Total sliding distance induced by  $NW$  waves during  $T_L$  is obtained by

$$s_{ttl} = NW \left\{ \int_0^{H_{20}} s \cdot P_{nb0}(H_0) dH_0 + \int_{H_{10}}^{\infty} s \cdot P_{b0}(H_0) dH_0 \right\} \quad (35)$$

in which  $s$  is the sliding distance induced by a single wave with  $H_0$  and  $\bar{T}_{1/3}$ . Breaking or non-breaking property of the waves must be carefully considered in the calculations from Eq.(9) to Eq.(26).

Applying one year  $H_{1/3}$  and  $\bar{T}_{1/3}$ , PDF of the one year total sliding distances  $P_{s1}(s_1)$  is obtained in which  $s_1$  is the one year total sliding distance.

#### Numerical simulations

Horikawa et al. (1989) reported about the properties of existing breakwaters in Japan. The present study used almost the average properties of the existing breakwaters along the Sea of Japan coast. The properties used in the calculations were listed in Table 3. Specific gravity of the caisson is assumed to be 2.8. Two different water depth cases are used in the simulations.



| Case  | 1     | 2      |
|-------|-------|--------|
| $h$   | 15m   | 20m    |
| $d$   | 10.5m | 13.5m  |
| $d_a$ | 1.5m  | 1.5m   |
| $h_c$ | 6m    | 6m     |
| $B$   | 6m    | 8m     |
| $W$   | 9~12m | 10~15m |
| $d_m$ | 3m    | 5m     |
| $\mu$ | 0.6   | 0.6    |

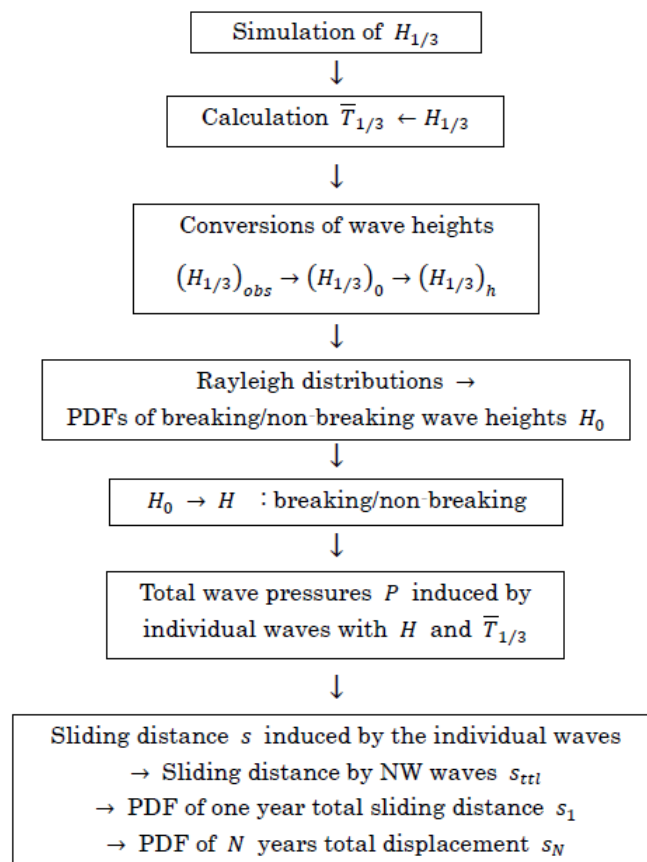


Figure 9. Flow of calculations.

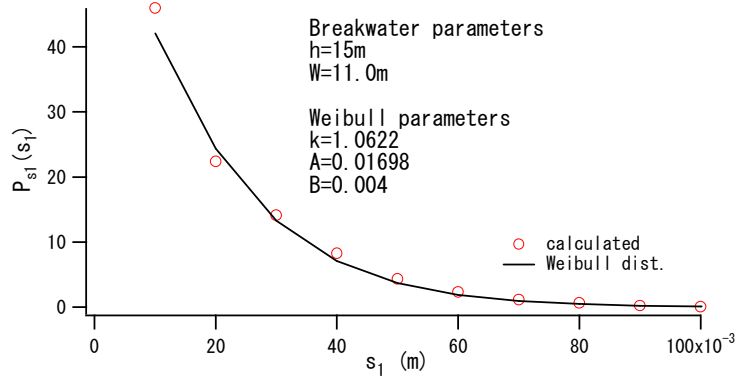
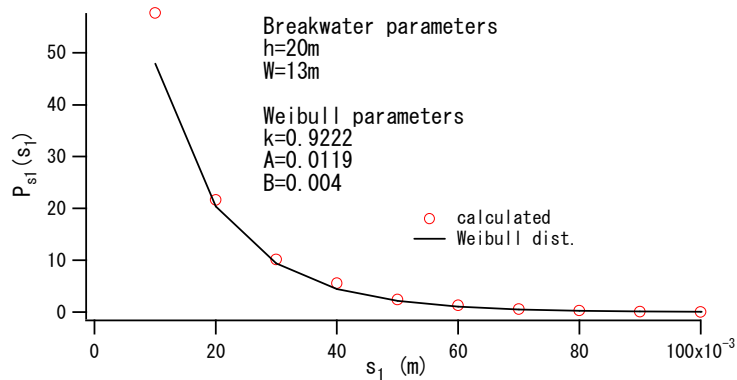
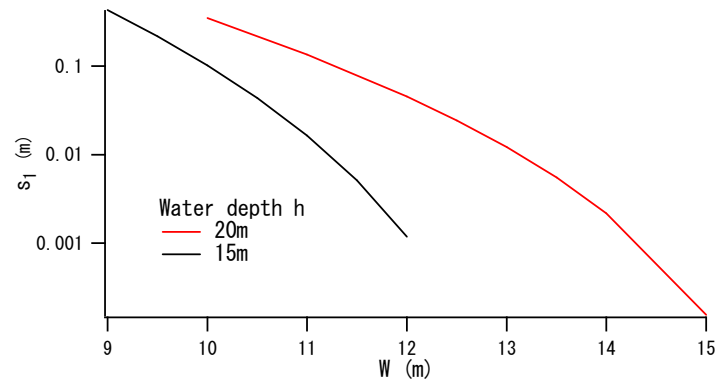
Figure 10. PDF of the one year total sliding distances  $s_1$ Figure 11. PDF of the one year total sliding distances  $s_1$ Figure 12. Relation between the average  $s_1$  and the breakwater thickness.

Figure 9 shows the flow of the calculations. Figures 10 (case 1) and 11 (Case 2) show the PDFs of the one year total sliding distances  $s_1$ . Water depth and breakwater thicknesses are shown in the figures. 10000 years  $H_{1/3}$  simulations were conducted. Figure 12 show the relation between the average of  $s_1$  and the breakwater thickness  $W$ .

One year sliding distance  $s_1$  is given by one year summation of  $s_{tll}$  (Eq.(35)). If the wave climates characteristics are independent every year, PDF of two years total sliding distance  $p_{s_2}(s_2)$  is derived as,

$$P_{s_2}(s_2) = \int_0^{s_2} P_{s_1}(s_1) P_{s_1}(s_2 - s_1) ds_1 \quad (36)$$

PDF of the  $N$  year total sliding distance  $s_N$  is given as

$$P_{s_N}(s_N) = \int_0^{s_N} P_{s_1}(s_1) P_{s(N-1)}(s_N - s_1) ds_1 \quad (37)$$

in which  $P_{s(N-1)}$  is the PDF of  $N - 1$  years total sliding distances. Repeated calculations of Eq.(37), PDF of the arbitral year siding distances can be derived from  $P_{s_1}(s_1)$ . Figures 13 and 14 show the

$P_{s_N}(s_N)$  for every 10 years in each case. Water depths and the breakwater thicknesses are shown in the figures. Sliding distance after  $N$  years of in-service period is given as

$$s_N = \sum_{i=1}^N s_{1i} \tag{38}$$

in which  $s_{1i}$  ( $i = 1, \dots, N$ ) is the one year total sliding distance of the  $i$ -th year. If each year  $s_{1i}$  is independent and  $N$  is sufficiently large,  $P_{s_N}(s_N)$  can be approximated by a normal distribution (law of large numbers).

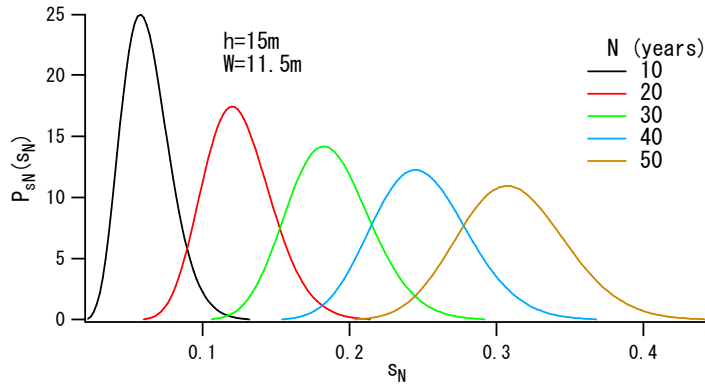


Figure 13.  $P_{s_N}(s_N)$  for every 10 years (Case 1)

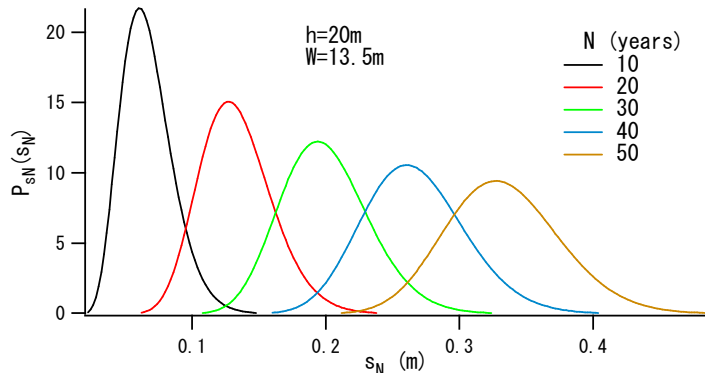


Figure 14.  $P_{s_N}(s_N)$  for every 10 years (Case 2)

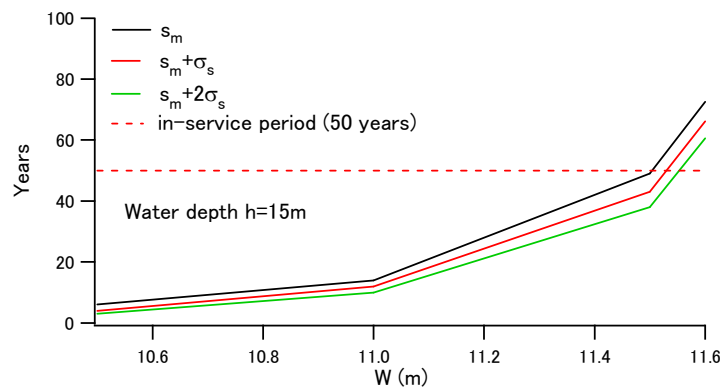


Figure 15. Relation between the breakwater thicknesses and the elapsed years until the total sliding distances exceed 0.3m.

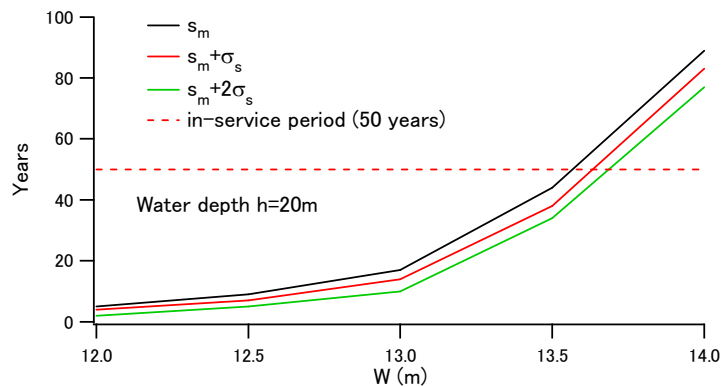


Figure 16. Relation between the breakwater thicknesses and the elapsed years until the total sliding distances exceed  $0.3m$ .

Japanese new guideline indicates that the performance of the composite breakwater is maintained unless the sliding distance exceeds  $0.3m$ . Figures 15 (Case 1) and 16 (Case 2) show the relation between the breakwater thicknesses and the elapsed years until the total sliding distances exceed  $0.3m$ . Three representative values  $s_m$ ,  $s_m + \sigma_s$  and  $s_m + 2\sigma_s$  of  $P_{sN}(s_N)$  are used in which  $s_m$  and  $\sigma_s$  are the mean and the standard deviation of  $P_{sN}(s_N)$  (Fig.13, 14). These figures show that  $W$  must be larger than  $12m$  (Case 1) and  $14m$  (Case 2) if there is no plan to repair its during the in-service period (50 years :  $s_m + 2\sigma_s$ , for example). Figure 17 shows the relations between  $s_N$  and elapsed years for each case (Case 1,  $W = 11.5m$  ; Case 2,  $W = 13.0m$  :  $s_m + 2\sigma_s$ ). Horizontal line in the figure shows the  $0.3m$ . Necessary maintenance time can be read in this figure.

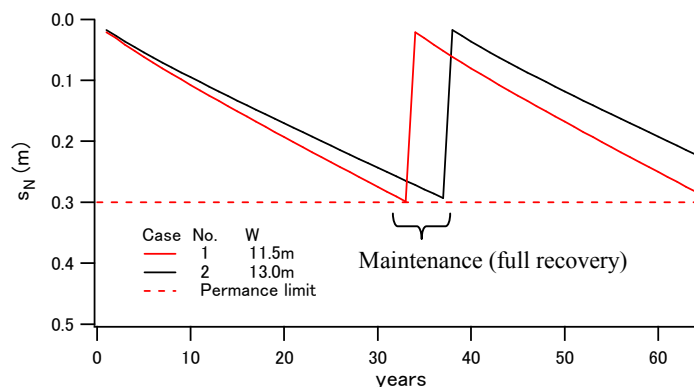


Figure 17. Relations between  $s_m + 2\sigma_s$  and elapsed years for each case (Case 1,  $W=11.5m$  ; Case 2,  $W=13.0m$ ).

### Remarks

Present study shows the scheme to simulate the statistical properties of the sliding distance of the composite breakwater applying the wave climate statistics. Two average type breakwaters installed in different water depths were used as examples in the simulations. Numerically simulated yearly change of the PDF of sliding distances and the statistical representative values such as the average, average+standard-deviation and average+2×standard-deviation are shown. Maintenance timings are also shown for two breakwater thicknesses during their in-service years.

The model to estimate the sliding distance of the breakwater is one of the very few examples that can be applied immediately to the performance design scheme. Many existing physical models mainly studied the process until the damage start. Very few studies showed the information after the damage take place. To activate the application of the new design scheme, accumulation of the information on the progress after damages may be important. New physical modeling on the damage progress is expecting. If there is sufficient information, effective Life Cycle Management of the coastal structures will be possible from the planning stage.

### REFERENCES

Goda, Y. (1974): A new method of wave pressure calculation for the design of composite breakwater, *proc. 14<sup>th</sup> ICCE*, 1702-1720.

- Goda, Y. (1975): Irregular wave deformation in the surf zone, *Coastal Engineering in Japan*, **18**, 13-26.
- Goda, Y. (2010): Random seas and design of maritime structures (3<sup>rd</sup> ed.), *World Scientific*, 708pp.
- Horikawa, H., K. Kanda and T. Horike (1989): Statistical data analysis on caisson composite type breakwater, *Tech. Note of PHRI*, **644**, 3-34. (in Japanese)
- Ito, Y, M. Fujishima and T. Kitatani (1971): On the stability of breakwaters, *Coastal Eng. In Japan*, **14**, 53-61.
- Kimura, A. T. Ota (2012): Statistical estimation of wave climates in a monsoon region, *Proc. 33<sup>rd</sup> ICCE, Management 20*, 1-15.
- Kimura, A. T. Ota (2013): Statistical properties of wave climate and its applications, *Proc. Coastal Eng.* **68**, I\_116-I\_120. (in Japanese), Micro properties of wave climate statistics and its applications, *Proc. 34<sup>th</sup> ICCE* (2014). (poster, in printing)
- Kimura, A. T. Ota (2014): Statistical property of combined wave climates along the Sea of Japan coast, *Proc. Coastal Eng.* **69**. (in printing, in Japanese)
- Ministry of Land Infrastructure and Transportation (2007): Technical standards of the harbor facilities and the commentaries, Vol. 1, 477pp.
- NOWPHAS: <http://www.mlit.go.jp/kowan/nowphas/>
- Shimosako, K. and S. Takahashi (1994): Calculation of expected sliding distance of composite breakwaters, *Proc. Coastal Eng.* **41**, 756-760. (in Japanese, English explanation appears in Goda (2010))
- Shimosako, K. and S. Takahashi (1998): Reliability design method of composite breakwaters using expected sliding distance, *Rept. PHRI* **37**(3), 3-30. (in Japanese, English explanation appears in Goda (2010))
- Tanimoto, K., K. Furukawa and H. Nakamura (1996): Fluid resistance of upright section of composite breakwater against sliding and new model of sliding distance estimation, *Proc Coastal Eng.* **43**, 846-850. (in Japanese, English explanation appears in Goda (2010))